ⓒ 应用数学和力学编委会, ISSN 1000-0887

含圆孔功能梯度压电材料板的力电耦合三维解析解*

张友源[1]，　范慧朵[1]，　沈璐璐[1]，　杨　博[1,2]

（1. 浙江理工大学 建筑工程学院，杭州 310018；
2. 浙江建设职业技术学院 建筑工程学院，杭州 311231）

（我刊编委陈伟球推荐）

摘要： 在推广后的 England-Spencer 功能梯度板理论基础上，该研究进一步将功能梯度弹性材料推广到了功能梯度压电材料，研究了含有圆孔无限大横观各向同性功能梯度压电材料板在机械荷载作用下的三维响应.该板理论将三维问题转化为二维问题，利用复变函数解法，通过求解四个解析函数获得具体边值问题的三维解析解.针对在无穷远处受机械荷载作用的含圆孔功能梯度压电材料板，利用边界条件确定了四个解析函数的具体表达形式.通过数值算例讨论了材料参数沿板厚方向呈指数函数梯度变化时，边界条件和相关参数对圆孔边上三维应力的影响.该解析方法可为分析功能梯度压电板的三维孔口问题提供有效解析求解手段.

关　键　词： 功能梯度压电材料；　圆孔；　力电耦合；　复变函数；　解析解
中图分类号： O343.8　　**文献标志码：** A　　DOI：10.21656/1000-0887.460016

3D Analytical Solutions of Mechatronic Coupling for Functionally Graded Piezoelectric Material Plates With a Circular Hole

ZHANG Youyuan[1]，　FAN Huiduo[1]，　SHEN Lulu[1]，　YANG Bo[1,2]

（1. *School of Civil Engineering and Architecture*, *Zhejiang Sci-Tech University*, *Hangzhou* 310018, *P.R.China*;
2. *Construction Engineering School*, *Zhejiang College of Construction*, *Hangzhou* 311231, *P.R.China*）

（Recommended by CHEN Weiqiu, M.AMM Editorial Board）

Abstract: Based on the extended England-Spencer functionally graded plate theory, the functionally graded elastic material (FGM) was extended to functionally graded piezoelectric material (FGPM) and the responses of the transversely isotropic FGPM plate containing a circular hole were investigated. By virtue of this theory, a 3D

* **收稿日期：** 2025-01-24；**修订日期：** 2025-03-24
基金项目： 国家自然科学基金(11872336)
作者简介： 张友源(2000—)，男，硕士生(E-mail：1161321979@qq.com)；
范慧朵(1999—)，女，硕士生(E-mail：19857129053@163.com)；
沈璐璐(1990—)，女，副教授，博士(E-mail：lulushen@zstu.edu.cn)；
杨博(1979—)，男，教授，博士(通讯作者. E-mail：youngbo@zstu.edu.cn).
引用格式： 张友源，范慧朵，沈璐璐，杨博. 含圆孔功能梯度压电材料板的力电耦合三维解析解[J]. 应用数学和力学，2025，**46**(11)：1416-1428.

boundary value problem can be transformed into a 2D one. The 3D analytical solution was obtained from 4 analytical functions based on the complex variable function method. For a FGPM plate with a circular hole and subjected to mechanical loads, the specific expressions of the 4 analytical functions were determined according to the boundary conditions. Numerical examples were presented to discuss the effects of boundary conditions and relevant parameters on the 3D stresses along the circular hole edge with the material parameters varying exponentially along the plate thickness. The analytical method provides an effective tool for accurate analysis of 3D hole-related issues in functionally graded piezoelectric plates.

Key words: functionally graded piezoelectric material; circular hole; mechatronic coupling; complex function; analytic solution

0 引　　言

功能梯度材料(FGM)是一种新型的非均质复合材料,其材料组分在空间上可以设计为连续梯度变化,使得材料的宏观性能也具有连续梯度变化的特征[1].压电材料因其卓越的机电耦合特性,被广泛应用于传感器和执行器等器件[2].为了克服压电材料层间界面和裂纹处的应力集中问题,人们将功能梯度概念应用于压电材料,从而发展出了功能梯度压电材料(FGPM)[3].这种新型材料可以通过材料组分的梯度变化优化应力分布,进而有效降低应力集中,显著提升压电器件或结构的稳定性和可靠性,目前在航空航天、生物医学[4]等多个高端领域有着广泛的潜在应用价值.

由于使用功能的需要,含有开孔的压电材料板结构被应用于诸多器件或工程领域.目前,国内外学者已经采用多种研究方法分析了孔洞对压电材料电弹场的影响[5-15].例如,Liang 等[5]利用特殊的边界元方法和 Green 函数,对含孔洞圆形压电板进行数值模拟分析,获得了在多种载荷条件下含孔洞无限压电板的精确解析解.Rao 等[6]基于扩展的 Stroh 理论体系处理了含孔洞压电板在远场任意耦合的力电荷载作用下的二维问题.蔡斌和周立明[7]提出了一种基于单元的力电耦合非均匀光滑有限元法来分析含圆孔 FGPM 板的二维问题.孟广伟等[8]提出了含孔 FGPM 板的力电耦合无网格 Galerkin 法,研究了孔边环向应力分布及力电集中的二维问题.Nguyen 等[9]结合有限元法和高阶剪切变形理论,研究了含孔 FGPM 板的二维平面问题,探讨了孔隙率、外部电压和材料参数等因素对板的电-机械振动响应的影响.Miao 和 Li[10]通过自然边界积分方程和区域分解法,研究了含圆孔压电板在给定位移和电势边界条件下的二维平面问题.王鑫特等[11]采用非局部应变梯度理论结合谐波解法,建立了多孔 FGPM 纳米壳体的波传播控制方程,并推导出了尺度相关的特征方程,通过数值方法研究了波数、尺度参数、孔隙率、梯度指数及电压对波传播特性的影响.Xu 和 Wang[12]基于横向各向同性压电板的精细理论,得到了含圆孔的无限大压电板受无穷远处弯矩作用时的解析解,给出了孔边弯矩、应力和电位移集中因子的闭式表达式.复变函数法能够将二维问题转化为复变量表达,结合保角变换技术,形成了一套解析研究孔口应力集中问题的成熟求解体系.例如,刘淑红等[13]采用复变函数的方法,研究了含有椭圆孔洞的压电材料在无限远处受力电荷载作用的平面问题.此外,Sasaki 等[14]、Kumari 等[15]也通过复变函数的方法对此类问题进行了研究.据笔者了解,目前对于含孔洞压电材料板问题的研究大多集中在二维问题上,关于含圆孔 FGPM 板的三维问题的研究并不充分.

England 和 Spencer[16]基于三维弹性理论提出了一种新的板理论,获得了表面应力自由条件下,各向同性功能梯度材料板的三维解析解,并结合复变函数求解了无限大板中的双轴应力问题等.笔者[17]利用该板理论研究了含孔口无限大横观各向同性功能梯度板的三维平衡问题.在此基础上,本文进一步将功能梯度弹性材料拓展到了 FGPM,给出了在远端机械荷载作用下,含圆孔 FGPM 板应力场的三维解析解.

1 基 本 理 论

1.1 基本方程

考虑一个含有圆孔的无限大横观各向同性 FGPM 板,如图 1 所示.xOy 面是各向同性面,z 轴方向为极化方向.

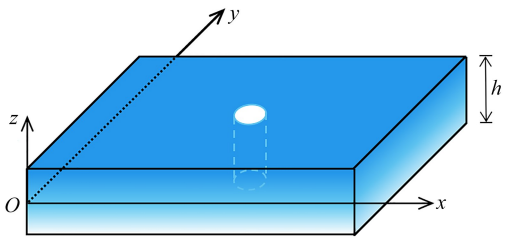

图 1 含圆孔无限大 FGPM 板示意图

Fig. 1 Schematic diagram of an infinite FGPM material plate with a circular hole

不考虑体积力时,力学平衡方程为

$$\tau_{xy,x}+\sigma_{y,y}+\tau_{yz,z}=0,\ \sigma_{x,x}+\tau_{xy,y}+\tau_{xz,z}=0,\ \tau_{zx,x}+\tau_{zy,y}+\sigma_{z,z}=0, \tag{1}$$

式中下标“,”表示对其后的变量求导数.

不考虑自由电荷密度,Gauss 电平衡方程为

$$D_{x,x}+D_{y,y}+D_{z,z}=0. \tag{2}$$

横观各向同性压电弹性体的本构方程[18]为

$$\begin{cases}\sigma_x=c_{11}u_{,x}+c_{12}v_{,y}+c_{13}w_{,z}+e_{31}\Phi_{,z},\ \sigma_y=c_{12}u_{,x}+c_{11}v_{,y}+c_{13}w_{,z}+e_{31}\Phi_{,z},\\ \tau_{zy}=c_{44}(v_{,z}+w_{,y})+e_{15}\Phi_{,y},\ \tau_{zx}=c_{44}(u_{,z}+w_{,x})+e_{15}\Phi_{,x},\ \tau_{xy}=c_{66}(u_{,y}+v_{,x}),\end{cases} \tag{3}$$

$$\begin{cases}D_x=e_{15}(u_{,z}+w_{,x})-\varepsilon_{11}\Phi_{,x},\\ D_y=e_{15}(v_{,z}+w_{,y})-\varepsilon_{11}\Phi_{,y},\\ D_z=e_{31}u_{,x}+e_{31}v_{,y}+e_{33}w_{,z}-\varepsilon_{33}\Phi_{,z},\end{cases} \tag{4}$$

其中, c_{ij} 为材料的弹性常数, e_{ij} 为压电常数, ε_{ij} 为介电常数.对于 FGPM,这些常数均为坐标 z 的函数, Φ 为电势.

考虑如下形式的位移场[19]:

$$\begin{cases}u(x,y,z)=\bar{u}(x,y)+F(z)\Delta_{,x}+A(z)\bar{w}_{,x}+B(z)\nabla^2\bar{w}_{,x},\\ v(x,y,z)=\bar{v}(x,y)+F(z)\Delta_{,y}+A(z)\bar{w}_{,y}+B(z)\nabla^2\bar{w}_{,y},\\ w(x,y,z)=\bar{w}(x,y)+G(z)\Delta+C(z)\nabla^2\bar{w}+D(z),\end{cases} \tag{5}$$

式中 $A(z),B(z),C(z),D(z),F(z),G(z)$ 为关于 z 的待定函数,且

$$\Delta=\Delta(x,y)=\bar{u}_{,x}+\bar{v}_{,y},\ \nabla^2=\partial^2/\partial x^2+\partial^2/\partial y^2. \tag{6}$$

参照上述位移场的模式,假设电势场沿板厚按如下形式分布

$$\Phi(x,y,z)=\Phi_1(z)\Delta+\Phi_2(z)\nabla^2\bar{w}+\Phi_0(z), \tag{7}$$

式中 $\Phi_0(z),\Phi_1(z)$ 和 $\Phi_2(z)$ 为关于 z 的待定函数.

将式(5)和(7)代入式(3)和(4),得到板的三维应力和电位移表达式:

$$\begin{cases}\sigma_x=(c_{12}+c_{13}G'+e_{31}\Phi_1')\Delta+c_{13}D'+e_{31}\Phi_0'+(c_{12}A+c_{13}C'+e_{31}\Phi_2')\nabla^2\bar{w}+\\ \qquad c_{12}(F\nabla^2\Delta+B\nabla^4\bar{w})+2c_{66}(\bar{u}_{,x}+F\Delta_{,xx}+A\bar{w}_{,xx}+B\nabla^2\bar{w}_{,xx}),\\ \sigma_y=(c_{12}+c_{13}G'+e_{31}\Phi_1')\Delta+c_{13}D'+e_{31}\Phi_0'+(c_{12}A+c_{13}C'+e_{31}\Phi_2')\nabla^2\bar{w}+\\ \qquad c_{12}(F\nabla^2\Delta+B\nabla^4\bar{w})+2c_{66}(\bar{v}_{,y}+F\Delta_{,yy}+A\bar{w}_{,yy}+B\nabla^2\bar{w}_{,yy}),\\ \sigma_z=(c_{13}+c_{33}G'+e_{33}\Phi_1')\Delta+c_{33}D'+e_{33}\Phi_0'+\\ \qquad (c_{13}A+c_{33}C'+e_{33}\Phi_2')\nabla^2\bar{w}+c_{13}(F\nabla^2\Delta+B\nabla^4\bar{w}),\\ \tau_{zy}=c_{44}(A'+1)\bar{w}_{,y}+[c_{44}(F'+G)+e_{15}\Phi_1]\Delta_{,y}+[c_{44}(B'+C)+e_{15}\Phi_2]\nabla^2\bar{w}_{,y},\\ \tau_{zx}=c_{44}(A'+1)\bar{w}_{,x}+[c_{44}(F'+G)+e_{15}\Phi_1]\Delta_{,x}+[c_{44}(B'+C)+e_{15}\Phi_2]\nabla^2\bar{w}_{,x},\\ \tau_{xy}=c_{66}(\bar{u}_{,y}+\bar{v}_{,x}+2F\Delta_{,xy}+2A\bar{w}_{,xy}+2B\nabla^2\bar{w}_{,xy}),\end{cases} \tag{8}$$

$$\begin{cases} D_x = e_{15}(A'+1)\bar{w}_{,x} + [e_{15}(F'+G) - \varepsilon_{11}\Phi_1]\Delta_{,x} + [e_{15}(B'+C) - \varepsilon_{11}\Phi_2]\nabla^2\bar{w}_{,x}, \\ D_y = e_{15}(A'+1)\bar{w}_{,y} + [e_{15}(F'+G) - \varepsilon_{11}\Phi_1]\Delta_{,y} + [e_{15}(B'+C) - \varepsilon_{11}\Phi_2]\nabla^2\bar{w}_{,y}, \\ D_z = (e_{31} + e_{33}G' - \varepsilon_{33}\Phi_1')\Delta + (e_{31}A + e_{33}C' - \varepsilon_{33}\Phi_2')\nabla^2\bar{w} + \\ \quad e_{31}(F\nabla^2\Delta + B\nabla^4\bar{w}) + e_{33}D' - \varepsilon_{33}\Phi_0', \end{cases} \tag{9}$$

式中上标“′”表示对变量 z 求导数.

将式(8)和(9)代入式(1)和(2),并令

$$\begin{cases} [c_{44}(A'+1)]' = 0,\ (c_{13} + c_{33}G' + e_{33}\Phi_{11}')' = 0,\ (e_{31} + e_{33}G' - \varepsilon_{33}\Phi_{11}')' = 0, \\ c_{11} + c_{13}G' + e_{31}\Phi_{11}' + [c_{44}(F'+G) + e_{15}\Phi_1]' = c_{66}\kappa_1, \\ c_{11}A + c_{13}C' + e_{31}\Phi_2' + [c_{44}(B'+C) + e_{15}\Phi_2]' = c_{66}\kappa_2, \\ c_{44}(A'+1) + (c_{13}A + c_{33}C' + e_{33}\Phi_{22}')' = 0, \\ e_{15}(A'+1) + (e_{31}A + e_{33}C' - \varepsilon_{33}\Phi_2')' = 0, \end{cases} \tag{10}$$

可得

$$\begin{cases} (\kappa_1\Delta + \kappa_2\nabla^2\bar{w})_{,x} - \Omega_{,y} = 0,\ (\kappa_1\Delta + \kappa_2\nabla^2\bar{w})_{,y} + \Omega_{,x} = 0, \\ H\kappa_3 + I\kappa_4 + (c_{33}D' + e_{33}\Phi_0')' = 0, \\ J\kappa_3 + K\kappa_4 + (e_{33}D' - \varepsilon_{33}\Phi_0')' = 0, \end{cases} \tag{11}$$

式中 κ_1 和 κ_2 为任意常数,且

$$\nabla^2\Delta = \kappa_3,\ \nabla^4\bar{w} = \kappa_4,\ \Omega = \bar{v}_{,x} - \bar{u}_{,y}, \tag{12}$$

$$\begin{cases} H = c_{44}(F'+G) + e_{15}\Phi_1 + (c_{13}F)', \\ I = c_{44}(B'+C) + e_{15}\Phi_2 + (c_{13}B)', \\ J = e_{15}(F'+G) - \varepsilon_{11}\Phi_1 + (e_{31}F)', \\ K = e_{15}(B'+C) - \varepsilon_{11}\Phi_2 + (e_{31}B)'. \end{cases} \tag{13}$$

由式(11)第 1 式和第 2 式可得

$$\nabla^2\Omega = 0,\ \nabla^2(\kappa_1\Delta + \kappa_2\nabla^2\bar{w}) = 0, \tag{14}$$

将式(12)代入式(14)第 2 式可得

$$\kappa_1\kappa_3 + \kappa_2\kappa_4 = 0. \tag{15}$$

1.2　确定未知函数表达式

若令 $\bar{u}$,$\bar{v}$ 和 $\bar{w}$ 为板的中面位移,由式(5)可得

$$A(0) = 0,\ B(0) = 0,\ C(0) = 0,\ D(0) = 0,\ F(0) = 0,\ G(0) = 0. \tag{16}$$

本文考虑在 FGPM 板上下表面具有如下边界条件:

$$z = \pm h/2:\ \sigma_z = 0,\ \tau_{zx} = \tau_{zy} = 0,\ D_z = 0. \tag{17}$$

积分式(10)和(11)并利用式(16)和(17)可以确定函数 $A(z)$,$B(z)$,$C(z)$,$D(z)$,$F(z)$,$G(z)$,$\Phi_0(z)$,$\Phi_1(z)$,$\Phi_2(z)$ 和常数 κ_1,κ_2,κ_3,κ_4 的表达式.具体表达式见附录 A.

2　无限多连通域下 FGPM 板的解析函数

2.1　复势函数基本解

引入复变量 $\zeta = x + \mathrm{i}y$, 此时板的中面位移可以表示为[17]

$$\begin{cases} \bar{u} + \mathrm{i}\bar{v} = \dfrac{\kappa_1 + 1}{\kappa_1 - 1}\phi(\zeta) - 2\dfrac{\kappa_2}{\kappa_1}[\beta(\zeta) + \zeta\overline{\beta'(\zeta)}] - \overline{\psi(\zeta)} - \zeta\overline{\phi'(\zeta)}, \\ \bar{w} = \alpha(\zeta) + \overline{\alpha(\zeta)} + \bar{\zeta}\beta(\zeta) + \zeta\overline{\beta(\zeta)}. \end{cases} \tag{18}$$

将式(18)代入式(5)和(7)可得用四个解析函数表示板内任一点的位移和电势表达式:

$$\begin{cases} u(x,y,z)+\mathrm{i}v(x,y,z)=\dfrac{\kappa_1+1}{\kappa_1-1}\phi(\zeta)-\zeta\overline{\phi'(\zeta)}-\overline{\psi(\zeta)}-2\left(\dfrac{\kappa_2}{\kappa_1}+z\right)[\beta(\zeta)+\zeta\overline{\beta'(\zeta)}]-\\ \qquad 2z\overline{\alpha'(\zeta)}+\dfrac{4}{\kappa_1-1}F(z)\overline{\phi''(\zeta)}-8\left[\dfrac{\kappa_2}{\kappa_1}F(z)-B(z)\right]\overline{\beta''(\zeta)},\\ w(x,y,z)=\alpha(\zeta)+\overline{\alpha(\zeta)}+\bar{\zeta}\beta(\zeta)+\zeta\overline{\beta(\zeta)}+\dfrac{2}{\kappa_1-1}G(z)[\phi'(\zeta)+\overline{\phi'(\zeta)}]-\\ \qquad 4\left[\dfrac{\kappa_2}{\kappa_1}G(z)-C(z)\right][\beta'(\zeta)+\overline{\beta'(\zeta)}]+D(z),\\ \Phi(x,y,z)=\dfrac{2}{\kappa_1-1}\Phi_1(z)[\phi'(\zeta)+\overline{\phi'(\zeta)}]+\\ \qquad 4\left[\Phi_2(z)-\dfrac{\kappa_2}{\kappa_1}\Phi_1(z)\right][\beta'(\zeta)+\overline{\beta'(\zeta)}]+\Phi_0(z). \end{cases} \tag{19}$$

进一步地,将式(18)代入式(8)和(9),并对应力和电位移在板厚方向上进行积分处理可得

$$\begin{cases} N_x+N_y=a_1[\phi'(\zeta)+\overline{\phi'(\zeta)}]+4a_2[\beta'(\zeta)+\overline{\beta'(\zeta)}],\\ M_x+M_y=-b_1[\phi'(\zeta)+\overline{\phi'(\zeta)}]+4b_2[\beta'(\zeta)+\overline{\beta'(\zeta)}],\\ N_y-N_x+2\mathrm{i}N_{xy}=a_1[\bar{\zeta}\phi''(\zeta)+\psi'(\zeta)]+4a_2\bar{\zeta}\beta''(\zeta)+2a_6\alpha''(\zeta)-a_5\phi'''(\zeta)-a_7\beta'''(\zeta),\\ M_y-M_x+2\mathrm{i}M_{xy}=a_6[\bar{\zeta}\phi''(\zeta)+\psi'(\zeta)]+b_6\bar{\zeta}\beta''(\zeta)+b_7\alpha''(\zeta)-b_5\phi'''(\zeta)-b_8\beta'''(\zeta),\\ Q_{xz}-\mathrm{i}Q_{yz}=Q_{z1}\phi''(\zeta)+Q_{z2}\beta''(\zeta),\ D_{xn}-\mathrm{i}D_{yn}=D_{z1}\phi''(\zeta)+D_{z2}\beta''(\zeta),\\ E_{xn}-\mathrm{i}E_{yn}=E_{z1}\phi''(\zeta)+E_{z2}\beta''(\zeta), \end{cases} \tag{20}$$

式中 $D_{xn},D_{yn},E_{xn},E_{yn}$ 为电位移和电场强度在板厚方向上的积分,常数 $a_1,a_2,a_5,a_6,a_7,b_1,b_2,b_5,b_6,b_7,b_8,Q_{z1},Q_{z2},D_{z1},D_{z2},E_{z1},E_{z2}$ 的表达式见附录 B.

2.2 无限多连通域情况

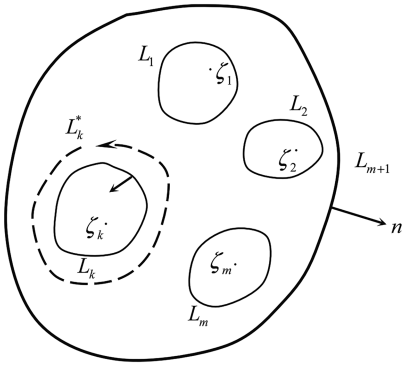

图 2 无限多连通区域的示意图

Fig. 2 Diagram of an infinitely connected region

考虑一个无限多连通域,如图 2 所示,该区域内部以轮廓集 $L_1,L_2,\cdots,L_k,\cdots,L_m$ 为界,外部轮廓集 L_{m+1} 趋于无穷远.在每个轮廓中取一个特定的点,如 $\zeta_1,\zeta_2,\cdots,\zeta_m$ 等.作闭围线 L_k^* 绕 L_k 且与其余围线均不相接触.将过 L_k 和 L_k^* 柱面所围成的那一块板分离出来进行研究.在过 L_k^* 柱面上作用有内应力,它们的主矢量和主矩分别记为 $X_k^*\boldsymbol{i}+Y_k^*\boldsymbol{j}+Z_k^*\boldsymbol{k}$ 和 $M_{Xk}^*\boldsymbol{i}+M_{Yk}^*\boldsymbol{j}+M_{Zk}^*\boldsymbol{k}$,以及它们的法向电位移和环向电场强度记为 $D_{\mathrm{n}k}^*$ 和 $E_{\mathrm{t}k}^*$.由电场环流定理[20]可知 $E_{\mathrm{t}k}^*=0$.

因此,该板的整体平衡条件为

$$\begin{cases} X_k+X_k^*=0,\ Y_k+Y_k^*=0,\ Z_k+Z_k^*=0,\\ M_{Xk}+M_{Xk}^*=0,\ M_{Yk}+M_{Yk}^*=0,\\ M_{Zk}+M_{Zk}^*=0,\ D_{\mathrm{n}k}+D_{\mathrm{n}k}^*=0,\ E_{\mathrm{t}k}=0. \end{cases} \tag{21}$$

考虑位移场和电势场的唯一性,在无限远处 FGPM 板的内力、内力矩、电位移和电势大小应该为有限值,利用式(20)和(21)可得四个解析函数的具体表达式:

$$\begin{cases} \alpha(\zeta)=[\kappa_7(X-\mathrm{i}Y)+\kappa_6(M_Y+\mathrm{i}M_X)]\zeta\ln\zeta+A\ln\zeta+\alpha_1\zeta+\alpha_2\zeta^2+\alpha_0(\zeta),\\ \beta(\zeta)=[\kappa_7(X+\mathrm{i}Y)+\kappa_6(M_Y-\mathrm{i}M_X)]\ln\zeta+\beta_1\zeta+\beta_0(\zeta),\\ \psi(\zeta)=[\kappa_{10}(X-\mathrm{i}Y)+\kappa_{11}(M_Y+\mathrm{i}M_X)]\ln\zeta+\psi_1\zeta+\psi_0(\zeta),\\ \phi(\zeta)=\kappa_5(X+\mathrm{i}Y)\ln\zeta+\phi_1\zeta+\phi_0(\zeta), \end{cases} \tag{22}$$

式中常数 $\kappa_5,\kappa_6,\kappa_7,\kappa_9,\kappa_{10}$ 和 κ_{11} 的表达式见附录 C; $\alpha_1,\alpha_2,\beta_1,\phi_1$ 和 ψ_1 为复常数且

$$\begin{cases}(X,Y,Z,M_X,M_Y,A)=\sum\limits_{k=1}^{m}(X_k,Y_k,Z_k,M_{Xk},M_{Yk},A_k),\\ [\alpha_0(\zeta),\beta_0(\zeta),\phi_0(\zeta),\psi_0(\zeta)]=[\alpha_0,\beta_0,\phi_0,\psi_0]+\sum\limits_{n=1}^{\infty}[\alpha_{-n},\beta_{-n},\phi_{-n},\psi_{-n}]\zeta^{-n},\end{cases}\tag{23}$$

其中 $\alpha_0(\zeta),\beta_0(\zeta),\phi_0(\zeta),\psi_0(\zeta)$ 是无穷远处的全纯函数.

将式(22)代入式(20),并令 $|\zeta|\to\infty$,可得无穷远处 FGPM 板的内力、内力矩、电位移和电场强度表达式:

$$\begin{cases}N_x^\infty+N_y^\infty=2a_1\mathrm{Re}\,\phi_1+8a_2\mathrm{Re}\,\beta_1,\ M_x^\infty+M_y^\infty=-2b_1\mathrm{Re}\,\phi_1+8b_2\mathrm{Re}\,\beta_1,\\ N_y^\infty-N_x^\infty+2\mathrm{i}N_{xy}^\infty=4a_6\alpha_2+a_1\psi_1,\ M_y^\infty-M_x^\infty+2\mathrm{i}M_{xy}^\infty=2b_7\alpha_2+a_6\psi_1,\\ Q_{xz}^\infty-\mathrm{i}Q_{yz}^\infty=0,\ D_{xn}^\infty-\mathrm{i}D_{yn}^\infty=0,\ E_{xn}^\infty-\mathrm{i}E_{yn}^\infty=0,\end{cases}\tag{24}$$

且

$$\begin{cases}\begin{Bmatrix}\mathrm{Re}\,\phi_1\\ \mathrm{Re}\,\beta_1\end{Bmatrix}=\dfrac{1}{8(a_1b_2+a_2b_1)}\begin{bmatrix}4b_2 & -4a_2\\ b_1 & a_1\end{bmatrix}\begin{Bmatrix}N_x^\infty+N_y^\infty\\ M_x^\infty+M_y^\infty\end{Bmatrix},\\ \begin{Bmatrix}\alpha_2\\ \psi_1\end{Bmatrix}=\dfrac{1}{2(2a_6^2-a_1b_7)}\begin{bmatrix}a_6 & -a_1\\ -2b_7 & 4a_6\end{bmatrix}\begin{Bmatrix}N_x^\infty-N_y^\infty+2\mathrm{i}N_{xy}^\infty\\ M_x^\infty-M_y^\infty+2\mathrm{i}M_{xy}^\infty\end{Bmatrix}.\end{cases}\tag{25}$$

2.3　利用孔边界条件求解解析函数

考虑 FGPM 板内的圆孔为电不可导通的自由圆孔,在圆孔边界 $r=a$ 处的边界条件为

$$N_r(a,\theta)-\mathrm{i}N_{r\theta}(a,\theta)=0,\ M_r(a,\theta)=0,\ Q_{rz}(a,\theta)+\frac{\partial M_{r\theta}(a,\theta)}{a\partial\theta}=0,\ \int_{-h/2}^{h/2}D_r(a,\theta,z)\,\mathrm{d}z=0.\tag{26}$$

直角坐标系与圆柱坐标系之间的物理量变换关系为

$$\begin{cases}N_r+N_\theta=N_x+N_y,\ M_r+M_\theta=M_x+M_y,\\ N_\theta-N_r+2\mathrm{i}N_{r\theta}=(N_y-N_x+2\mathrm{i}N_{xy})\mathrm{e}^{2\mathrm{i}\theta},\ M_\theta-M_r+2\mathrm{i}M_{r\theta}=(M_y-M_x+2\mathrm{i}M_{xy})\mathrm{e}^{2\mathrm{i}\theta},\\ D_r=D_x\cos\theta+D_y\sin\theta.\end{cases}\tag{27}$$

根据式(26)和(27),将式(22)代入式(20)并利用等式 $\zeta=a\mathrm{e}^{\mathrm{i}\theta}$ 可得

$$2(a_1\mathrm{Re}\,\phi_1+4a_2\mathrm{Re}\,\beta_1)+(a_1\psi_{-1}+2a_6A)a^{-2}=0,\tag{28}$$

$$2a_1\bar{C}a^{-1}\kappa_1/(\kappa_1-1)=0,\tag{29}$$

$$(a_1C+4a_2B)a^{-1}+(a_1\psi_{-2}-2a_6\alpha_{-1}+a_5C+a_7B)a^{-3}=0,\tag{30}$$

$$-(a_1\bar{\phi}_{-1}+4a_2\bar{\beta}_{-1})a^{-2}-(a_1\psi_1+4a_6\alpha_2)=0,\tag{31}$$

$$-3[(a_1\phi_{-1}+4a_2\beta_{-1})a^{-2}+(2a_5\phi_{-1}+2a_7\beta_{-1}-a_1\psi_{-3}+4a_6\alpha_{-2})a^{-4}]=0,\tag{32}$$

$$-n(a_1\bar{\phi}_{-n}+4a_2\bar{\beta}_{-n})a^{-n-1}=0,\tag{33}$$

$$-(n+2)\{n(a_1\phi_{-n}+4a_2\beta_{-n})a^{-n-1}+[2(n+1)a_6\alpha_{-n-1}+n(n+1)(a_5\phi_{-n}+a_7\beta_{-n})-a_1\psi_{-n-2}]a^{-n-3}\}=0,\tag{34}$$

$$2(-b_1\mathrm{Re}\,\phi_1+4b_2\mathrm{Re}\,\beta)+(a_6\mathrm{Re}\,\psi_{-1}+b_7A)=0,\tag{35}$$

$$[4b_2B+(a_6\kappa_1/(\kappa_1-1)-b_1)C]a^{-1}+(a_6\psi_{-2}-b_7\alpha_{-1}+b_5C+b_8B)a^{-3}=0,\tag{36}$$

$$-2[(-b_1+a_6)\phi_{-1}+(4b_2+b_6)\beta_{-1}]a^{-2}-(2b_7\bar{\alpha}_2+a_6\bar{\psi}_1)-3[2(b_5\phi_{-1}+b_8\beta_{-1})+2b_7\alpha_{-2}-a_6\psi_{-3}]a^{-4}=0,\tag{37}$$

$$-n\{[-2b_1+(n+1)a_6]\phi_{-n}+[8b_2+(n+1)b_6]\beta_{-n}\}a^{-n-1}-(n+2)[n(n+1)(b_5\phi_{-n}+b_8\beta_{-n})+(n+1)b_7\alpha_{-n-1}-a_6\psi_{-n-2}]a^{-n-3}=0,\tag{38}$$

$$[(4b_2-2Q_{z2})B-(a_6\kappa_1/(\kappa_1-1)+b_1+2Q_{z1})C]a^{-2}+$$

$$(a_6\psi_{-2} - b_7\alpha_{-1} + b_5C + b_8B)a^{-4} = 0, \tag{39}$$

$$2[(Q_{z1} - a_6)\phi_{-1} + (Q_{z2} - b_6)\beta_{-1}]a^{-3} + (2b_7\bar{\alpha}_2 + a_6\bar{\psi}_1)a^{-1} - 3[2(b_5\phi_{-1} + b_8\beta_{-1}) + 2b_7\alpha_{-2} - a_6\psi_{-3}]a^{-5} = 0, \tag{40}$$

$$(n+1)\{n\{[2Q_{z1} - (n+1)a_6]\phi_{-n} + [2Q_{z2} - (n+1)b_6]\beta_{-n}\}a^{-n-2} - (n+2)[n(n+1)(b_5\phi_{-n} + b_8\beta_{-n}) + (n+1)b_7\alpha_{-n-1} - a_6\psi_{-n-2}]a^{-n-4}\} = 0, \tag{41}$$

$$(CD_{z1} + BD_{z2})a^{-2} = 0, \tag{42}$$

$$n(n+1)(D_{z1}\bar{\phi}_{-n} + D_{z2}\bar{\beta}_{-n})a^{-n-2} = 0, \tag{43}$$

其中

$$C = \kappa_5(X + \mathrm{i}Y),\ B = \kappa_7(X + \mathrm{i}Y) + \kappa_6(M_Y - \mathrm{i}M_X). \tag{44}$$

利用式(42)和(43)可确定函数 Φ_1 和 Φ_2 的表达式.常数 $\mathrm{Re}\,\phi_1$,$\mathrm{Re}\,\beta_1$,α_2 和 ψ_1 可以由式(25)确定.与内力、位移和电位移无关的常数 α_1,α_0,β_0,ϕ_0,ψ_0 可以设为零.ψ_{-1} 和常数 A 可以从式(28)和(35)中确定.ϕ_{-1},β_{-1},α_{-2} 和 ψ_{-3} 可以由式(31)、(32)、(37)和(40)可确定.由式(30)、(36)和(39)可以推得 α_{-1} 和 ψ_{-2} 为零,由式(33)、(34)、(38)和(41)可以推得 ϕ_{-n},β_{-n},α_{-n-1} 和 ψ_{-n-2}($n = 2,3,\cdots$) 都为零.因此式(22)可以简化为

$$\begin{cases}\alpha(\zeta) = A\ln\zeta + \alpha_2\zeta^2 + \alpha_{-2}\zeta^{-2},\ \phi(\zeta) = \mathrm{Re}(\phi_1\zeta) + \phi_{-1}\zeta^{-1},\\ \beta(\zeta) = \mathrm{Re}(\beta_1\zeta) + \beta_{-1}\zeta^{-1},\ \psi(\zeta) = \psi_1\zeta + \psi_{-1}\zeta^{-1} + \psi_{-3}\zeta^{-3}.\end{cases} \tag{45}$$

3 数值算例与分析

3.1 结果验证

为了验证本文解答的准确性,首先将横观各向同性 FGPM 板退化为横观各向同性均匀材料压电板(以下简称为横观各向同性 HPM 板).在板无穷远处施加力矩 $M_x = M_0$, 得到圆孔边的无量纲力矩结果 M_θ/M_0,并与文献[12]对比,如表 1 所示.另外,还将横观各向同性 FGPM 板退化为横观各向同性 FGM 板,将孔边的无量纲力矩结果 M_θ/M 与文献[17]进行比较,如表 2 所示,此时板内没有力电耦合效应.

表 1 横观各向同性 HPM 板孔边的力矩 M_θ/M_0 对比

Table 1 Torque ratios M_θ/M_0 at the edge of a hole in a transversely isotropic HPM plate

θ	0	0.523	1.046	1.569	2.092	2.615	3.141
the present	−0.083	0.462	1.561	2.130	1.561	0.462	−0.083
ref. [12]	−0.092	0.445	1.542	2.105	1.542	0.445	−0.092

表 2 横观各向同性 FGM 板孔边的力矩 M_θ/M 对比

Table 2 Torque ratios M_θ/M at the edge of a hole in a transversely isotropic FGM plate

θ	0	0.523	1.046	1.569	2.092	2.615	3.141
the present	0.224	0.667	1.552	1.996	1.552	0.667	0.224
ref. [17]	0.224	0.667	1.552	1.996	1.552	0.667	0.224

通过以上对比可以发现,本文在退化处理后的结果与文献[12]存在一定的误差.误差的出现主要源于两者的理论基础不同:文献[12]是基于板理论进行研究,而本文则是基于弹性理论.而且,最大误差在 5% 以内,比较结果可以接受.此外,文献[17]与本文采用了相同的理论基础,本文的退化结果与文献[17]的结果一致,符合预期.

3.2 参数分析

接下来考虑受无穷远处机械荷载作用时,圆孔边上的环向应力受压电效应和梯度效应的影响.取板厚 $h = 0.015$ m,孔径 $a = 0.01$ m, 考虑材料参数沿板厚方向变化规律为

$$c_{ij} = c_{ij}^0P^n,\ e_{ij} = e_{ij}^0P^n,\ \varepsilon_{ij} = \varepsilon_{ij}^0P^n,\qquad i,j = 1,2,\cdots,6,\ n = 1,2,3,4, \tag{46}$$

式中 c_{ij}^0,e_{ij}^0,ε_{ij}^0 分别为 $z = -h/2$ 处的材料弹性常数、压电常数和介电常数; P^n 为材料参数沿板厚方向的变化形式,其中

$$\begin{cases} P^1 = \mathrm{e}^{(0.5+z/h)\lambda},\ P^2 = (0.5+z/h)^{\lambda}+1, \\ P^3 = \sin\left[(0.5+z/h)\dfrac{\pi}{2}\right]\lambda+1,\ P^4 = (0.5+z/h)\lambda+1, \end{cases} \tag{47}$$

取 λ 为梯度因子,表示材料的不均匀程度;当 $\lambda = 0$ 时,FGPM 板退化为 HPM 板.以 PZT-4 陶瓷为例,取材料参数为[21]

$$c_{11}^0 = 1.39\times10^{11}\ \mathrm{N/m^2},\ c_{12}^0 = 7.78\times10^{10}\ \mathrm{N/m^2},\ c_{13}^0 = 7.43\times10^{10}\ \mathrm{N/m^2},$$
$$c_{33}^0 = 1.15\times10^{11}\ \mathrm{N/m^2},\ c_{44}^0 = 2.56\times10^{10}\ \mathrm{N/m^2},$$
$$e_{15}^0 = 12.7\ \mathrm{C/m^2},\ e_{31}^0 = -5.2\ \mathrm{C/m^2},\ e_{33}^0 = 15.1\ \mathrm{C/m^2},$$
$$\varepsilon_{11}^0 = 6.5\times10^{-9}\ \mathrm{F/m},\ \varepsilon_{33}^0 = 5.6\times10^{-9}\ \mathrm{F/m}.$$

除非特别说明,当讨论沿环向分布时,取板中面上的孔边位置进行分析;当研究沿板厚方向分布时,取孔边 $\theta = \pi/2$ 位置处进行分析.引入无量纲量 $\sigma_\alpha = h\cdot\sigma_\theta/N_x^\infty$,$\sigma_\beta = h^2\cdot\sigma_\theta/(4M_x^\infty)$.

3.3　算例分析

考虑 FGPM 板材料参数沿板厚方向的变化形式为 P^1,分析其在无穷远处受不同机械荷载作用时孔边的三维应力分布特征,并与相同条件下的 FGM 板进行对比分析.具体算例分析如下.

算例 1　单向拉伸

图 3 给出了 FGM 板和 FGPM 板在无穷远处受 $N_x^\infty = 1$ N 作用时,圆孔边环向应力的分布情况.从图 3(b)中可以看出: ① 孔边环向应力沿环向分布先增大后减小,且在 $\theta = \pi/2$ 处达到最大值; ② 相比于 FGM 板,FGPM 板的孔边应力集中效应减小.图 3(c)表明: ① FGPM 板内孔边环向应力分布沿板厚方向从下而上先增大后减小,且梯度因子越大,应力梯度变化越剧烈,应力集中效应也越强; ② HPM 板内孔边环向应力沿板厚方向呈均匀分布; ③ 相比于 FGM 板,FGPM 板孔边的最大应力可降低 20.1%.

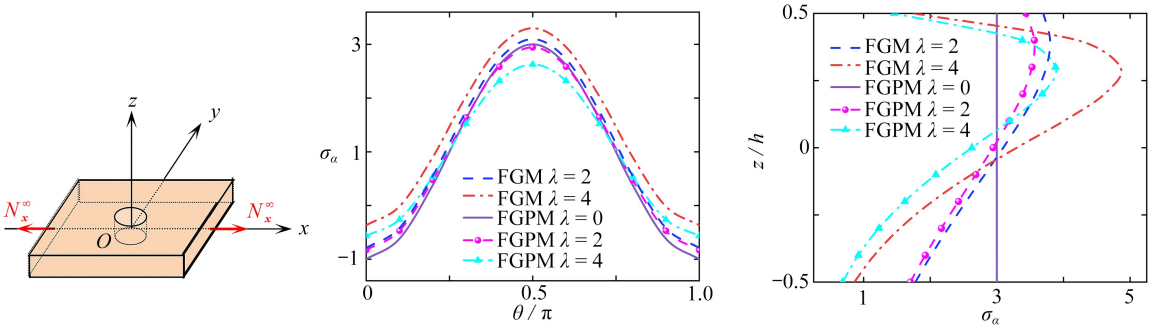

(a) 板受单向拉伸作用示意图　(b) 沿孔边环向分布图　(c) 沿板厚方向分布图

(a) Diagram of a plate under uniaxial tension　(b) Circumferential distribution along the hole edge　(c) Distribution along the thickness direction of the hole

图 3　无穷远处受单向拉伸作用时孔边无量纲环向应力分布

Fig. 3　Distributions of dimensionless circumferential stresses around the hole in a plate under uniaxial tension at infinity

注　为了解释图中的颜色,读者可以参考本文的电子网页版本,后同.

算例 2　单边弯曲

图 4 给出了 FGM 板和 FGPM 板在无穷远处受 $M_x^\infty = 1$ N·m 作用时,圆孔边环向应力的分布情况.从图 4(b)中可以看出: ① 孔边环向应力沿环向分布先增大后减小,在 $\theta = \pi/2$ 处达到最大值; ② 相比于 FGM 板,FGPM 板的孔边应力集中效应减小; ③ HPM 板内孔边中面处无环向应力.图 4(c)表明: ① 板内孔边环向应力在上表面处集中,且梯度因子越大,应力集中效应越大; ② HPM 板内孔边环向应力沿板厚方向呈线性分布; ③ FGPM 板相比于 FGM 板,孔边应力集中效应减弱的程度随着梯度因子的增大而增大,最大应力可降低 14.4%.

算例 3　扭转

图 5 给出了 FGM 板和 FGPM 板在无穷远处受 $M_{xy}^\infty = 1$ N·m 作用时,圆孔边环向应力的分布情况.从图 5

(b)中可以看出：① 孔边环向应力沿环向呈正弦函数分布，在 $\theta=\pi/4$ 和 $\theta=3\pi/4$ 处达到峰值；② HPM 板内孔边中面处无环向应力.图 5(c)表明：① 孔边环向应力在上表面处集中，且梯度因子越大，应力集中效应越强；② HPM 板内孔边环向应力曲线沿板厚方向呈线性分布；③ 相比于 FGM 板，FGPM 板的孔边应力集中效应微弱增强.

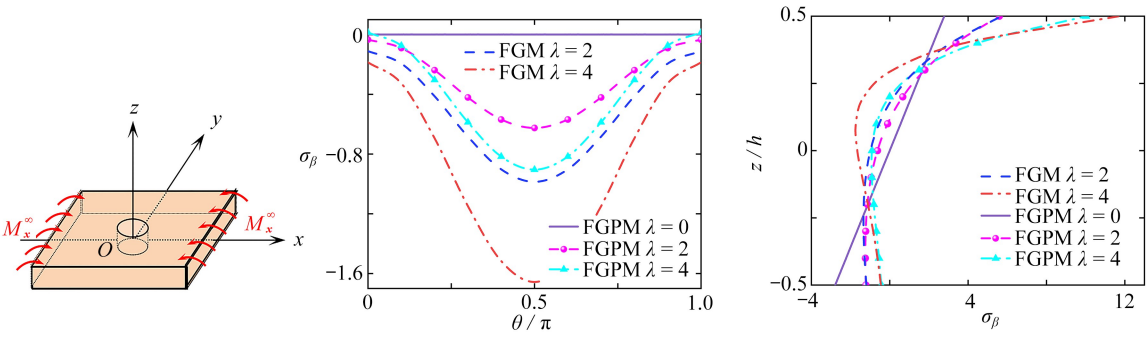

(a) 板受单边弯曲作用示意图
(a) Diagram of a plate under unilateral bending

(b) 沿孔边环向分布图
(b) Circumferential distribution along the hole edge

(c) 沿板厚方向分布图
(c) Distribution along the thickness direction of the hole

图 4 无穷远处受单边弯曲作用时孔边无量纲环向应力分布

Fig. 4 Distributions of dimensionless circumferential stresses around the hole in a plate under unilateral bending at infinity

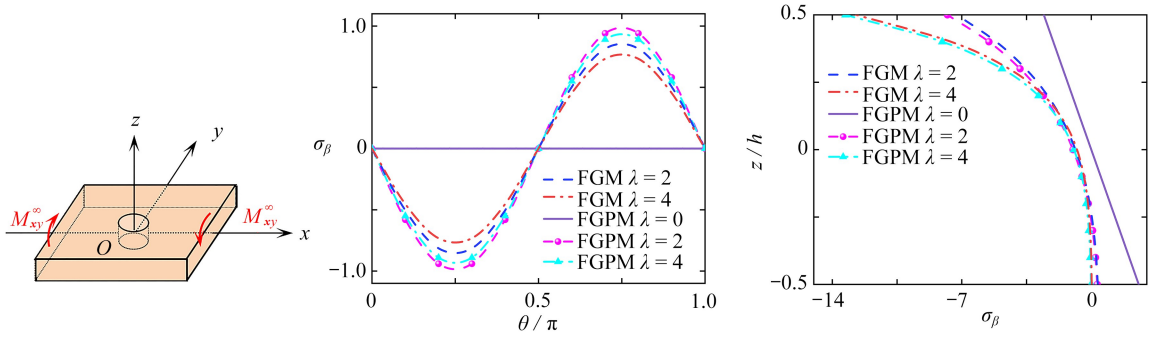

(a) 板受扭转作用示意图
(a) Diagram of a plate under torsion

(b) 沿孔边环向分布图
(b) Circumferential distribution along the hole edge

(c) $\theta=\pi/4$ 时沿板厚方向分布图
(c) Distribution along the thickness direction of the hole for $\theta=\pi/4$

图 5 无穷远处受扭转作用时孔边无量纲环向应力分布

Fig. 5 Distributions of dimensionless circumferential stresses around the hole in a plate under torsion at infinity

算例 4 双向拉伸

图 6 给出了 FGPM 和 FGM 板在无穷远处受 $N_x^\infty=1$ N 和 $N_y^\infty=1$ N 作用时，圆孔边环向应力的分布情况.从图 6(b)中可以看出：孔边应力沿环向呈均匀分布，但与 FGM 板相比，FGPM 板内孔边应力明显较小.图 6(c)表明：① 孔边应力在板厚方向上有两处集中区域，并且随着梯度因子的增大，应力集中效应也越强；② 与 FGM 板相比，FGPM 板的最大应力可降低 29.8%；③ HPM 板内孔边环向应力沿板厚方向呈均匀分布.

结合图 3 分析可得：与受单向拉伸作用相比，板在受双向拉伸作用时，孔边应力沿环向分布更均匀，沿板厚方向分布趋势更平缓，且应力集中效应明显更小，但 FGPM 板相比于 FGM 板的应力集中程度降低的幅度更大.

算例 5 双边弯曲

图 7 给出了 FGPM 和 FGM 板在无穷远处受 $M_x^\infty=1$ N·m 和 $M_y^\infty=1$ N·m 作用时，圆孔边环向应力的分布情况.从图 7(b)中可以看出，板内孔边应力沿环向呈均匀分布，相比于 FGM 板，FGPM 板内孔边的应力更小.从图 7(c)可以发现：① 孔边应力在上表面处集中，并且梯度因子越大，应力集中效应也越强；② FGPM 板相比于 FGM 板，最大应力可减少 8.9%；③ HPM 板内孔边应力沿板厚方向呈线性分布.

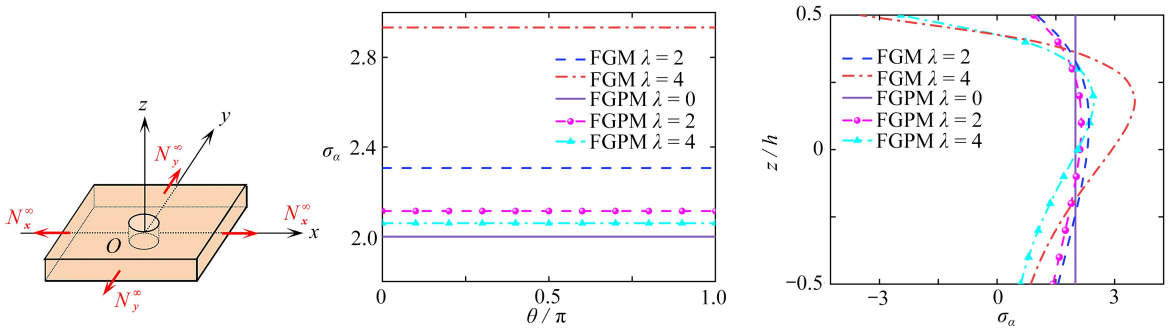

（a）板受双向拉伸作用示意图　（b）沿孔边环向分布图　（c）沿板厚方向分布图

（a）Diagram of a plate under biaxial tension　（b）Circumferential distribution along the hole edge　（c）Distribution along the thickness direction of the hole

图 6　无穷远处受双向拉伸作用时孔边无量纲环向应力分布

Fig. 6　Distributions of dimensionless circumferential stresses around the hole in a plate under biaxial tension at infinity

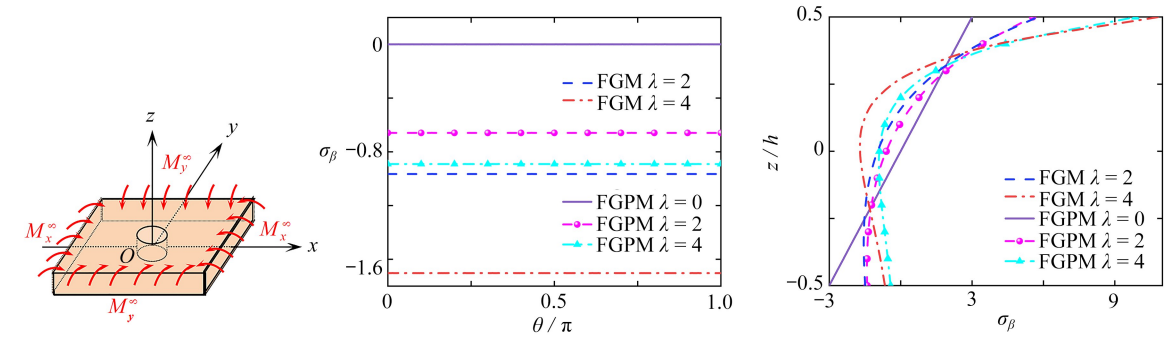

（a）板受双边弯曲作用示意图　（b）沿孔边环向分布图　（c）沿板厚方向分布图

（a）Diagram of a plate under bilateral bending　（b）Circumferential distribution along the hole edge　（c）Distribution along the thickness direction of the hole

图 7　无穷远处受双边弯曲作用时孔边无量纲环向应力分布

Fig. 7　Distributions of dimensionless circumferential stresses around the hole in a plate under bilateral bending at infinity

结合图 4 分析可得：与受单边弯曲作用相比，板在受双边弯曲作用时，孔边环向应力沿环向分布更均匀，沿板厚方向分布趋势相似，但应力集中效应明显更弱，FGPM 板相比于 FGM 板的应力集中程度降低的幅度也更小。

接下来，分析 FGPM 板在无穷远处受 $N_x^\infty = 1$ N 作用时，其材料参数沿板厚方向的四种梯度变化形式对孔边应力集中程度的影响。取梯度因子 $\lambda = 2$，以弹性常数 c_{11} 为例，材料参数沿板厚方向分布如图 8(a)所示。从图 8(b)和表 3 可以发现：① 在不同材料参数梯度变化形式下，孔边的应力分布规律呈现出明显差异；② 当材料参数呈现 P^1 指数分布时，孔边应力集中现象最为显著，而当材料参数为 P^4 线性分布时，应力集中现象相对较弱；③ FGPM 板相较于 FGM 板，孔边应力集中缓解的幅度受材料参数变化形式的影响。具体而言，在 P^1 指数分布情况下，FGPM 板的应力集中缓解的幅度远大于其他三种分布形式；而在 P^3 正弦分布时，其缓解幅度则相对较小。

表 3　材料参数的变化形式对孔边环向应力集中的影响

Table 3　The impacts of material parameter variations on circumferential stress concentrations around the hole

material parameter variation		P^1	P^2	P^3	P^4
max σ_α	FGM plate	3.801	3.618	3.408	3.348
	FGPM plate	3.567	3.565	3.363	3.285
magnitude of stress concentration relief of the FGPM plate compared to the FGM plate		6.16%	1.46%	1.32%	1.88%

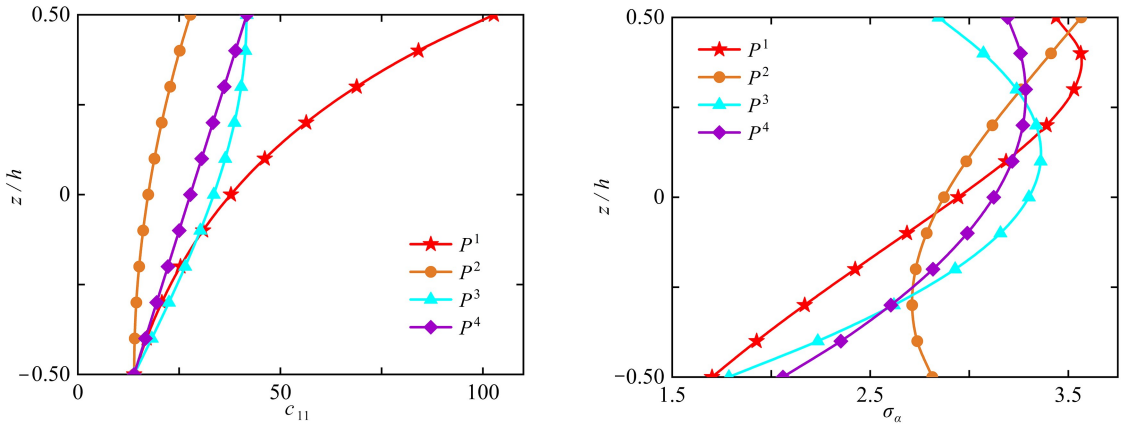

(a) 弹性常数 c_{11} 变化曲线 (b) 环向应力变化曲线

(a) Variations of elasticity constant c_{11} (b) Variation curves of the hoop stress

图 8 弹性常数和无量纲环向应力沿板厚方向变化曲线

Fig. 8 Variation of elastic constants and dimensionless hoop stress along the thickness

4 结 论

本文研究了含圆孔无限大横观各向同性 FGPM 板的力电耦合三维问题.将 England-Spencer 功能梯度板理论由弹性材料推广到压电材料,获得了受无穷远处机械荷载作用时的三维解析解.针对圆孔处的应力集中问题,进行了相关参数分析,通过与 HPM 板和 FGM 板的已有解答比较,证明了本文解答的有效性.数值算例给出了含孔 FGPM 板在无穷远处受不同机械荷载作用下,板内孔边环向应力的三维分布特征.结果表明,在承受远场机械载荷时,与 FGM 板相比,FGPM 板由于其力电耦合效应,孔边应力集中显著降低,降低的程度和材料参数的变化形式、板的梯度因子以及在无穷远处施加的机械荷载类型有关,最大应力降低的幅度可达 29.8%.因此,在实际工程中,通过调控边界载荷与材料梯度因子,能够有效控制并优化 FGPM 板中孔边的三维应力分布.本文给出的三维解析解可为含圆孔的功能梯度压电材料(或均匀分布的压电材料)器件研发或三维分析提供理论指导.

附 录 A

$$A(z) = -z,\ G(z) = -g_0^0(z) + G_0,\ C(z) = g_1^0(z) + C_0,$$
$$F(z) = \kappa_1 f_6(z) - f_5(z) + g_0^1(z) - \varphi_1(z) - (z + h/2)G_0 + F_0,$$
$$B(z) = \kappa_2 f_6(z) + f_4(z) - g_1^1(z) - \varphi_2(z) - (z + h/2)C_0 + B_0,$$
$$D(z) = 0,\ \Phi_0(z) = 0,$$

其中

$$A_0 = 0,\ G_0 = g_0^0(0),\ C_0 = -g_1^0(z),$$
$$F_0 = -\kappa_1 f_6(0) + f_5(0) - g_0^1(0) + \varphi_1(0) + (z + h/2)g_0^0(0),$$
$$B_0 = -\kappa_2 f_6(0) - f_4(0) + g_1^1(0) + \varphi_2(0) - (z + h/2)g_1^0(z),$$
$$g_i^n(z) = \int_{-h/2}^{z} (z-\xi)^n \xi^i \left(\frac{\varepsilon_{33} c_{13} + e_{33} e_{31}}{c_{33}\varepsilon_{33} + e_{33}^2} \right) \mathrm{d}\xi, \qquad i,n = 0,1,$$
$$g_6(z) = \int_{-h/2}^{z} c_{66}(\xi)\,\mathrm{d}\xi,\ p_i^n(z) = \int_{-h/2}^{z} (z-\xi)^n \xi^i \left(\frac{e_{31} c_{33} - e_{33} c_{13}}{c_{33}\varepsilon_{33} + e_{33}^2} \right) \mathrm{d}\xi, \qquad i,n = 0,1,$$
$$h_i^n(z) = \int_{-h/2}^{z} (z-\xi)^n \xi^i \left[c_{11}(\xi) - \frac{\varepsilon_{33} c_{13}^2 + 2 e_{33} e_{31} c_{13} - e_{31}^2 c_{33}}{c_{33}\varepsilon_{33} + e_{33}^2}(\xi) \right] \mathrm{d}\xi, \qquad i,n = 0,1,$$
$$f_5(z) = \int_{-h/2}^{z} h_0^0(\xi) c_{44}^{-1}(\xi)\,\mathrm{d}\xi,\ f_2(z) = g_0^1(z) - f_5(z),\ f_6(z) = \int_{-h/2}^{z} g_6(\xi) c_{44}^{-1}(\xi)\,\mathrm{d}\xi,\ f_4(z) = \int_{-h/2}^{z} h_1^0(\xi) c_{44}^{-1}(\xi)\,\mathrm{d}\xi,$$
$$\varphi_1(z) = \int_{-h/2}^{z} (p_0^0(\xi) + \Phi_{10}) c_{44}^{-1}(\xi) e_{15}(\xi)\,\mathrm{d}\xi,\ \varphi_2(z) = \int_{-h/2}^{z} (-p_1^0(0) + A_0 p_0^0(0) + \Phi_{20}) c_{44}^{-1}(\xi) e_{15}(\xi)\,\mathrm{d}\xi,$$

$$\kappa_1 = \frac{h_0^0(h/2)}{g_6(h/2)},\ \kappa_2 = \frac{-h_1^0(h/2)}{g_6(h/2)},\ \kappa_3 = \kappa_4 = 0.$$

附　录　B

$$a_1 = 4g_6(h/2),\ a_2 = \frac{2}{\kappa_1}[\kappa_2 g_6(h/2) + \kappa_1 g_7(h/2)],\ a_5 = \frac{16}{\kappa_1 - 1}R_1^1,\ a_6 = 4g_7(h/2),\ a_7 = 32\left(R_2^1 - \frac{\kappa_2}{\kappa_1}R_1^1\right),$$

$$b_1 = \frac{4}{\kappa_1 - 1}[\kappa_2 g_6(h/2) + g_7(h/2)],\ b_2 = 2\left[\frac{\kappa_2^2}{\kappa_1}g_6(h/2) + \frac{\kappa_2}{\kappa_1}g_7(h/2) - h_2^0(h/2) + g_8(h/2)\right],$$

$$b_5 = \frac{16}{\kappa_1 - 1}R_1^2,\ b_6 = \frac{8}{\kappa_1}[\kappa_1 g_8(h/2) + \kappa_2 g_7(h/2)],\ b_7 = 8g_8(h/2),\ b_8 = 32\left(R_2^2 - \frac{\kappa_2}{\kappa_1}R_1^2\right),\ b_6 = b_7 + 2\frac{\kappa_2}{\kappa_1}a_6,$$

$$Q_{z1} = \frac{4}{\kappa_1 - 1}\int_{-h/2}^{h/2}[\kappa_1 g_6(z) - h_0^0(z)]\mathrm{d}z,\ Q_{z2} = 8\int_{-h/2}^{h/2}\left[h_1^0(z) + \frac{\kappa_2}{\kappa_1}h_0^0(z)\right]\mathrm{d}z,$$

$$E_{z1} = -\frac{4}{\kappa_1 - 1}\int_{-h/2}^{h/2}\Phi_1\mathrm{d}z,\ E_{z2} = 8\int_{-h/2}^{h/2}\left(\frac{\kappa_2}{\kappa_1} - \Phi_2\right)\mathrm{d}z,$$

$$D_{z1} = \frac{4}{\kappa_1 - 1}\left\{\frac{e_{15}}{c_{44}}[\kappa_1 g_6(z) - h_0^0(z)] - \left(\frac{e_{15}^2}{c_{44}} + \lambda_{11}\right)[p_0^0(z) + \Phi_{10}]\right\}\mathrm{d}z,$$

$$D_{z2} = 8\int_{-h/2}^{h/2}\left\{\frac{e_{15}}{c_{44}}\left[h_1^0(z) + \frac{\kappa_2}{\kappa_1}h_0^0(z)\right] - \left(\frac{e_{15}^2}{c_{44}} + \lambda_{11}\right)\left[-p_1^0(0) - \frac{\kappa_2}{\kappa_1}p_0^0(z) + \Phi_{20} - \frac{\kappa_2}{\kappa_1}\Phi_{10}\right]\right\}\mathrm{d}z,$$

其中

$$g_7(z) = \int_{-h/2}^{z}c_{66}(\xi)\xi\mathrm{d}\xi,\ g_8(z) = \int_{-h/2}^{z}c_{66}(\xi)\xi^2\mathrm{d}\xi,$$

$$R_1^1 = \int_{-h/2}^{h/2}c_{66}(z)F(z)\mathrm{d}z,\ R_2^1 = \int_{-h/2}^{h/2}c_{66}(z)B(z)\mathrm{d}z,\ R_1^2 = \int_{-h/2}^{h/2}zc_{66}(z)F(z)\mathrm{d}z,\ R_2^2 = \int_{-h/2}^{h/2}zc_{66}(z)B(z)\mathrm{d}z.$$

附　录　C

$$\kappa_5 = \frac{\kappa_1 - 1}{2\pi a_1\kappa_1},\ \kappa_6 = \frac{1}{\pi(4b_2 + Q_{z2} - b_6)},\ \kappa_7 = -\frac{(\kappa_1 - 1)\left(-b_1 + Q_{z1} + a_6\dfrac{\kappa_1 + 1}{\kappa_1 - 1}\right)}{2\pi a_1\kappa_1(4b_2 + Q_{z2} - b_6)},$$

$$\kappa_9 = \frac{-4b_2 + Q_{z2} + b_6}{2\pi Q_{z2}(4b_2 + Q_{z2} - b_6)},\ \kappa_{10} = 2\frac{\kappa_2\kappa_7}{\kappa_1} - \frac{\kappa_9(\kappa_1 + 1)}{\kappa_1 - 1},\ \kappa_{11} = 2\frac{\kappa_2\kappa_6}{\kappa_1}.$$

参考文献(References):

[1] 宋晨晨, 严新锐, 张子傲, 等. 功能梯度材料制备技术研究进展[J]. 表面技术, 2022, **51**(12): 20-38.(SONG Chenchen, YAN Xinrui, ZHANG Ziao, et al. Research progress in manufacturing technology of functionally graded materials[J]. *Surface Technology*, 2022, **51**(12): 20-38. (in Chinese))

[2] SANG Y, PENG K, DING Z, et al. Environmental vibration energy collection technology based on piezoelectric and electromagnetic model[J]. *Mechanics of Advanced Materials and Structures*, 2022, **29**(25): 3595-3601.

[3] RUBIO W M, VATANABE S L, PAULINO G H. *Functionally Graded Piezoelectric Material Systems: a Multiphysics Perspective*[M]. Wiley-VCH, 2015.

[4] YUANX, SHI J, KANG Y, et al. Piezoelectricity, pyroelectricity, and ferroelectricity in biomaterials and biomedical applications[J]. *Advanced Materials*, 2024, **36**(3): e2308726.

[5] LIANG Y C, SUN Y P, WU L N. Hole problems in a circular piezoelectric plate[J]. *Transactions of the Canadian Society for Mechanical Engineering*, 2016, **40**(4): 491-500.

[6] RAO D K N, BABU M R, ALAMIREW A, et al. A general solution for electromechanical analysis of electroelastic composite plates with arbitrary holes[J]. *Heliyon*, 2024, **10**(15): e35272.

[7] 蔡斌, 周立明. 基于非均匀光滑有限元法的含圆孔功能梯度压电板应力和电场集中因子分析[J]. 中南大学学报(自然科学版), 2018, **49**(5): 1080-1086.(CAI Bin, ZHOU Liming. Analysis of stress and electric field concen-

tration in a functionally graded piezoelectric plate with a circular hole based on nonhomogeneous smoothed finite element method[J]. *Journal of Central South University* (*Science and Technology*), 2018, **49**(5): 1080-1086. (in Chinese))

[8] 孟广伟, 王晖, 周立明, 等. 含孔功能梯度压电材料板的力电耦合无网格伽辽金法[J]. 中南大学学报(自然科学版), 2015, **46**(11): 4015-4020. (MENG Guangwei, WANG Hui, ZHOU Liming, et al. Electromechanical element-free Galerkin method for functionally graded piezoelectric plate with circular hole[J]. *Journal of Central South University* (*Science and Technology*), 2015, **46**(11): 4015-4020. (in Chinese))

[9] NGUYEN L B, THAI C H, ZENKOUR A M, et al. An isogeometric Bézier finite element method for vibration analysis of functionally graded piezoelectric material porous plates[J]. *International Journal of Mechanical Sciences*, 2019, **157**: 165-183.

[10] MIAO X Y, LI G Q. Analysis of piezoelectric plates with a hole using nature boundary integral equation and domain decomposition[J]. *Engineering Analysis With Boundary Elements*, 2014, **40**: 71-77.

[11] 王鑫特, 刘娟, 胡彪, 等. 多孔功能梯度压电纳米壳中波传播特性[J]. 应用数学和力学, 2024, **45**(2): 197-207. (WANG Xinte, LIU Juan, HU Biao, et al. Wave propagation in functionally graded piezoelectric nanoshells [J]. *Applied Mathematics and Mechanics*, 2024, **45**(2): 197-207. (in Chinese))

[12] XU S P, WANG W. Bending of piezoelectric plates with a circular hole[J]. *Acta Mechanica*, 2009, **203**(3): 127-135.

[13] 刘淑红, 李延强, 沈英明. 含椭圆孔压电材料的电弹场[J]. 工程力学, 2012, **29**(12): 45-50. (LIU Shuhong, LI Yanqiang, SHEN Yingming. The electro-elastic fields of piezoelectric materials with an elliptic hole[J]. *Engineering Mechanics*, 2012, **29**(12): 45-50. (in Chinese))

[14] SASAKI T, SUZUKI T, HIRASHIMA K. Transversely isotropic piezoelectric materials with an arbitrarily shaped boundary[J]. *Acta Mechanica*, 2006, **184**(1): 217-230.

[15] KUMARI S, UPHADHYAY A K, SHUKLA K K. Stress analysis for an infinite plate with circular holes[J]. *Materials Today: Proceedings*, 2017, **4**(2): 2323-2332.

[16] ENGLAND A H, SPENCER A J M. Complex variable solutions for inhomogeneous and laminated elastic plates [J]. *Mathematics and Mechanics of Solids*, 2005, **10**(5): 503-539.

[17] YANG B, CHEN W Q, DING H J. 3D elasticity solutions for equilibrium problems of transversely isotropic FGM plates with holes[J]. *Acta Mechanica*, 2015, **226**(5): 1571-1590.

[18] CHEN W Q, LEE K Y. Alternative state space formulations for magnetoelectric thermoelasticity with transverse isotropy and the application to bending analysis of nonhomogeneous plates[J]. *International Journal of Solids and Structures*, 2003, **40**(21): 5689-5705.

[19] 沈璐璐, 蔡方圆, 杨博. 功能梯度压电板柱面弯曲的弹性力学解[J]. 应用数学和力学, 2023, **44**(3): 272-281. (SHEN Lulu, CAI Fangyuan, YANG Bo. Elasticity solutions for cylindrical bending of functionally graded piezoelectric material plates[J]. *Applied Mathematics and Mechanics*, 2023, **44**(3): 272-281. (in Chinese))

[20] SHADOWITZ A, SCOTT W T. The electromagnetic field[J]. *American Journal of Physics*, 1976, **44**(6): 611-616.

[21] DING H, CHEN W. *Three Dimensional Problems of Piezoelasticity*[M]. Huntington N Y: Nova Science Publishers, 2001.